View metadata, citation and similar papers at core.ac.uk
brought to you by CORE
provided by Archivio istituzionale della ricerca - Università di Trieste

OXFORD

Human Molecular Genetics, 2015, Vol. 24, No. 9 2641–2648

doi: 10.1093/hmg/ddv026
Advance Access Publication Date: 26 January 2015
Original Article

ORIGINAL ARTICLE

The p.Cys169Tyr variant of connexin 26 is not a polymorphism

Francesco Zonta[1], Giorgia Girotto[2], Damiano Buratto[1], Giulia Crispino[1,3], Anna Morgan[2], Khalid Abdulhadi[4], Moza Alkowari[5], Ramin Badii[5], Paolo Gasparini[2,6] and Fabio Mammano[1,3,7,*]

[1]Dipartimento di Fisica e Astronomia 'G. Galilei', Università di Padova, 35131 Padova, Italy, [2]Department of Medical, Surgical and Health Sciences, University of Trieste, 34100 Trieste, Italy, [3]Istituto Veneto di Medicina Molecolare, Fondazione per la Ricerca Biomedica Avanzata, 35129 Padova, Italy, [4]Audiology and Balance Unit, National Program for Early Detection of Hearing Loss, WH, Hamad Medical Corporation (HMC) Doha, Doha, Qatar, [5]Molecular Genetics Laboratory, Department of Laboratory of Medicine and Pathology, Hamad Medical Corporation (HMC), Doha, Qatar, [6]Medical Genetics, Institute for Maternal and Child Health-IRCCS 'Burlo Garofolo', Trieste, Italy and [7]CNR Institute of Cell Biology and Neurobiology, 00015 Monterotondo, Rome, Italy

*To whom correspondence should be addressed at: CNR-IBCN, Via E. Ramarini 32, 00015 Monterotondo (RM), Italy. Tel: +39 06 90091 207; Fax: +39 06 90091 260; Email: fabio.mammano@cnr.it

Downloaded from http://hmg.oxfordjournals.org/ by guest on September 28, 2015

Abstract

Mutations in the *GJB2* gene, which encodes the gap junction protein connexin 26 (Cx26), are the primary cause of hereditary prelingual hearing impairment. Here, the p.Cys169Tyr missense mutation of Cx26 (Cx26C169Y), previously classified as a polymorphism, has been identified as causative of severe hearing loss in two Qatari families. We have analyzed the effect of this mutation using a combination of confocal immunofluorescence microscopy and molecular dynamics simulations. At the cellular level, our results show that the mutant protein fails to form junctional channels in HeLa transfectants despite being correctly targeted to the plasma membrane. At the molecular level, this effect can be accounted for by disruption of the disulfide bridge that Cys169 forms with Cys64 in the wild-type structure (Cx26WT). The lack of the disulfide bridge in the Cx26C169Y protein causes a spatial rearrangement of two important residues, Asn176 and Thr177. In the Cx26WT protein, these residues play a crucial role in the intra-molecular interactions that permit the formation of an intercellular channel by the head-to-head docking of two opposing hemichannels resident in the plasma membrane of adjacent cells. Our results elucidate the molecular pathogenesis of hereditary hearing loss due to the connexin mutation and facilitate the understanding of its role in both healthy and affected individuals.

Received: December 10, 2014. **Revised and Accepted:** January 21, 2015

© The Author 2015. Published by Oxford University Press.
This is an Open Access article distributed under the terms of the Creative Commons Attribution Non-Commercial License (http://creativecommons.org/licenses/by-nc/4.0/), which permits non-commercial re-use, distribution, and reproduction in any medium, provided the original work is properly cited. For commercial re-use, please contact journals.permissions@oup.com

Introduction

Twenty-one genes in the human genome encode connexin proteins (indicated with the abbreviation Cx followed by their molecular weight in kiloDalton; e.g. Cx26 for the 26 kDa isomer) with similar structure (1). Connexins are post-translationally oligomerized to form hexameric assemblies, known as connexons or hemichannels, prior to membrane insertion either within the endoplasmic reticulum or in the trans-Golgi network. Connexin hemichannels are then trafficked to the plasma membrane where the head-to-head docking of two hemichannels from adjacent cells promotes the formation of an intercellular channel with a pore diameter typically >1 nm (2,3). Tens of thousands of such channels aggregate in a gap junction plaque, allowing cell-to-cell diffusion of ions and selected metabolites, including second messengers, amino acids, nucleotides and glucose (4–6). The importance of electrical and molecular signaling through gap junction channels is widely recognized (4,7). Plasma membrane hemichannels that remain undocked are thought to rest in a predominantly closed state. However, they may open transiently in response to a wide range of stimuli permitting the controlled release of cytoplasmic ATP, glutamate, NAD+, prostaglandin E2, glutathione and other paracrine messengers (7), which are also critical for intercellular communication and the regulation of key inflammatory responses (8).

Consistent with the widespread expression of connexins in virtually any organ, mutations leading to change in properties, regulation or expression of connexin-made channels (i.e. hemichannels and gap junction channels) have been implicated in a variety of human diseases, including neuropathies due to demyelination of peripheral axons, idiopathic atrial fibrillation, visceroatrial heterotaxia, cataracts, oculodentodigital dysplasia, skin disorders and hearing impairment. Up to 50% of prelingual hearing impairment cases, with peaks reaching 79% among Mediterraneans, have been linked to mutations in *GJB2*, the gene encoding Cx26. This 226-amino acid protein is highly expressed by non-sensory cells of the inner ear, together with structurally related connexin 30 (Cx30) (9,10). More than 200 *GJB2* mutations, typically autosomal recessive, have been linked to hereditary hearing loss (11,12). Cx26 is also expressed in the skin and 18 *GJB2* mutations, mostly autosomal-dominant (which typically produce functional hemichannels with aberrant properties), have been linked to syndromic deafness associated with dermatological manifestations that can be highly invalidating or disfiguring (13). The only structure resolved at near-atomic resolution (3.5 Å) is that of a (homomeric homotypic) gap junction channel formed by human Cx26 protomers (2).

Mutations of connexin expressing genes can affect connexin hemichannels or gap-junction channels in several ways. Thus, early truncation of the protein cause profound hearing loss, whereas missense mutations present more variable phenotypes since they can modify the trafficking, the docking between hemichannel, the permeation or conductance properties of the channels or their gating properties (14,15). However, assessing the pathogenic role of a mutation is not necessarily straightforward, and *GJB2* is no exception.

The p.Cys169Tyr variant of Cx26, first described by Azaiez *et al.* (16), provides an example in which the effects of a single point mutation have not been immediately understood. The lack of segregation with a hearing phenotype in some trios and large families prompted its classification as a polymorphism (17), and as such, it is currently listed in online databases (e.g. http://web.expasy.org/variant_pages/VAR_009968.html).

However, the p.Cys169Tyr allele has been recently singled out in a consanguineous Arabian family from the Middle East; based on the use of *in silico* predictor tools, p.Cys169Tyr has been assumed as causative (18). Here, we extended the analysis of this mutation in the attempt to clarify its possible role and controversial issues associated with the available data.

Results

Sanger sequencing analysis of two Qatari families (*a* and *b*) performed on the most common worldwide non-syndromic hereditary hearing loss genes (*GJB2, GJB6* and A1555G mitochondrial mutation) revealed the presence of the c.A506G mutation in the *GJB2* gene, which causes the substitution of a cysteine amino acid with a tyrosine residue at position 169 of the Cx26 protein (Cx26C169Y). Family *a*, previously described in (17), presented with partial lack of segregation of the p.Cys169Tyr mutation. Briefly, both parents (obligate carriers) showed normal hearing, while the four siblings presented moderate-to-severe hearing loss (Fig. 1). Three patients (II-1, II-2 and II-3) are homozygous for this allele, while Patient II-4, characterized by severe hearing loss, is heterozygous, lacking a second *GJB2* mutated allele. Similarly to Patient II-4 just described in Family a, also in Family *b* (a trio), the proband is heterozygous for this allele as well as the normal hearing father (17). Although this variant was described by several *in silico* predictor tools [i.e. MutationTaster (19), Polyphen-2 (20) and SIFT (21)] as highly damaging, there was no clear genotype–phenotype relationship in both families. To further understand these findings, the largest family (*a*) was included in a greatly extended screening of 18 Qatari families aimed at the identification of novel alleles/genes using Linkage analysis and whole-exome sequencing (WES). Linkage analysis (following an incomplete penetrance model) revealed a positive signal only on chromosome 13 in the *GJB2* region, while WES identified the p.Cys169Tyr mutation as the only possible causative allele. Within this large screening, another consanguineous trio (Family *c*) carrying the same surname and showing the same phenotype (moderate-to-severe sensorineural bilateral hearing loss) presented the p.Cys169Tyr mutation of Cx26 segregating with the disease. Considering that the Qatari population is organized in tribes, the presence of the same surname and the same disease strongly suggests that these two families are closely related to each other. Altogether these findings suggest a possible causative role of the p.Cys169Tyr variant of Cx26.

Cx26 immunolabeling performed in Hela cell transfectants suggest that Cx26C169Y mutant connexons fail to form gap junctional plaques

To understand at which level the p.Cys169Tyr mutation affects the Cx26 protein, we transiently transfected Hela DH cells with either wild-type or mutant constructs and performed immunostaining with antibodies against Cx26 (Fig. 2). In cells overexpressing Cx26WT proteins, gap junction plaques were seen at points of cell-to-cell contact, with limited intracellular staining. In contrast, in HeLa DH cells overexpressing mutant Cx26C169Y proteins, the immunofluorescence signal exhibited a predominantly diffuse and cytoplasmic localization, with limited staining at the plasma membrane level. The analysis of confocal through-focus image sequences (z-stacks) highlighted the presence of mature junctional plaques connecting adjacent cells in the Cx26WT transfectants (Fig. 2A–D). Plaques were not observed in the mutant transfectants (Fig. 2F–I). Altogether, these results suggest that a (fraction of the) Cx26C169Y hemichannels are correctly targeted to the plasma

Downloaded from http://hmg.oxfordjournals.org/ by guest on September 28, 2015

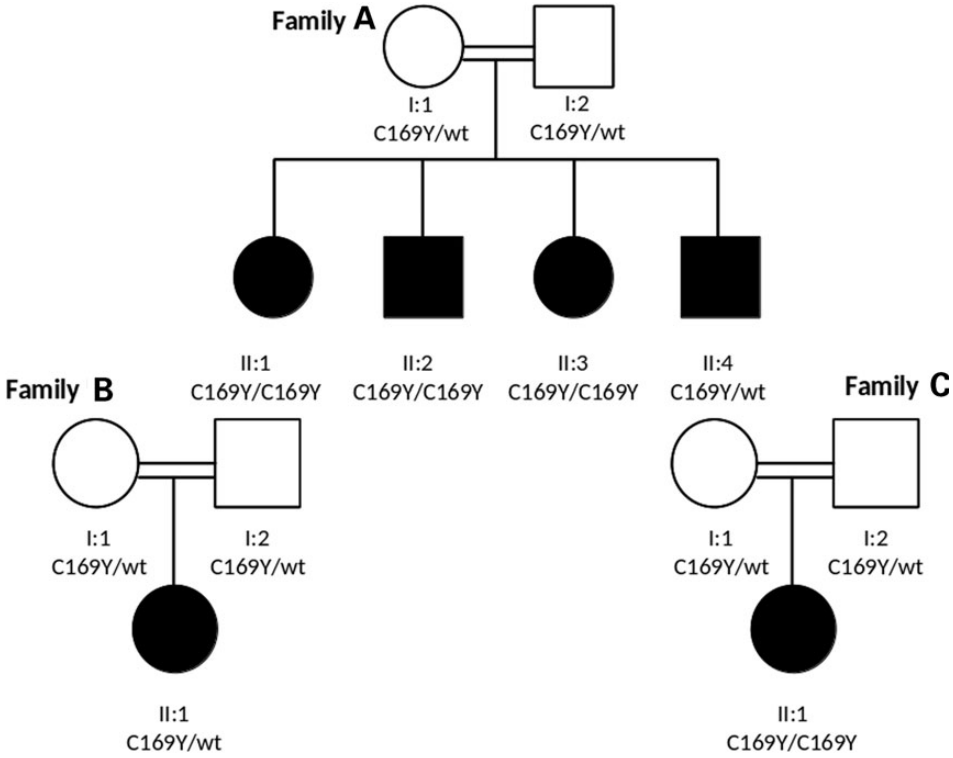

Figure 1. Pedigree of the families with indication of the phenotypes and the *GJB2* genotypes. Pedigree showing three families with Cys169Tyr variants. For Family *a*, affected individuals are: II:1 (Cys169Tyr/ Cys169Tyr), II:2 (Cys169Tyr /Cys169Tyr) II:3 (Cys169Tyr/Cys169Tyr) and II:4; (Cys169Tyr /wt); Family *b*: the proband is II:1 (Cys169Tyr /wt); Family *c*: the proband is II:1 (C169Y/C169Y). Note: (Cys169Tyr /Cys169Tyr), homozygous; (Cys169Tyr /wt), heterozygous; wt, wild-type.

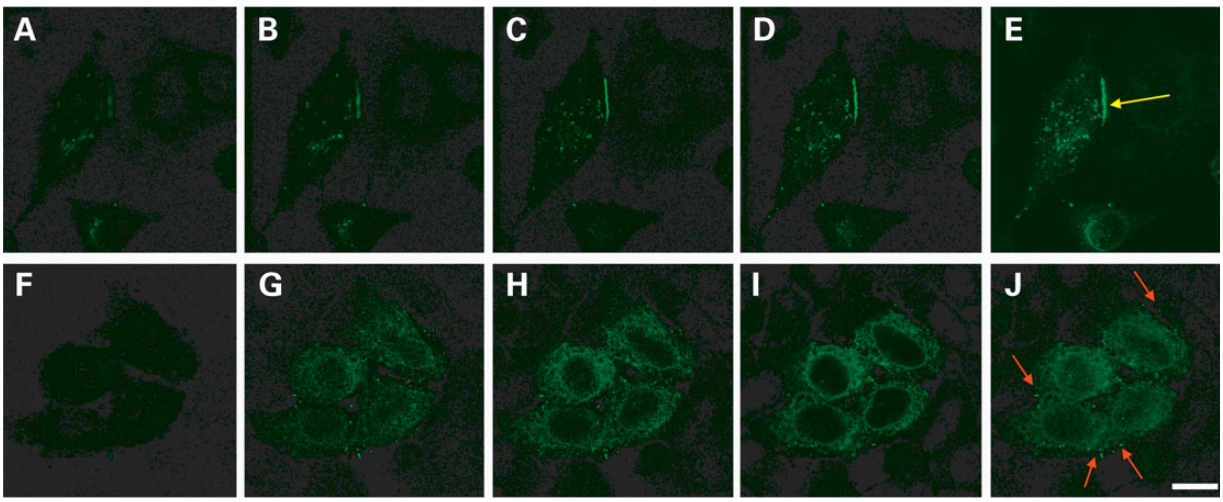

Figure 2. Cx26 immunostaining performed in Hela DH transfectants overexpressing Cx26WT (top), and Cx26C169Y (bottom) proteins. Through focus confocal image sequence (z-stack) taken at 0.5 µm intervals of Hela DH cells expressing Cx26WT (**A–D**) and Cx26C169Y (**F–I**) proteins and their respective maximal projection rendering (**E** and **J**). Yellow arrow points to representative gap junction plaque, whereas red arrows indicate immunoreaction signals at the cell plasma membrane level, which are most likely due to unpaired connexons. Scale bar, 10 µm.

membrane, but fail to dock to each other in neighboring cells, thus preventing the formation of gap junction channels.

Molecular dynamics simulations show significant alteration of the extra cellular domain in the Cx26C169Ymutant connexon

To corroborate the hypothesis that the p.Cys169Tyr mutation prevents the formation of Cx26 intercellular channels, we used molecular dynamics simulations (22–24). In the extracellular region of the Cx26WT protein, Cys169 forms a (strong covalent) disulfide bond with Cys64, which keeps the distance between the two sulfur atoms at 2.05 A. In the Cx26C169Y protein, the p.Cys169Tyr substitution makes the formation of this bond impossible and produces an alteration in the distance between residues 64 and 169 (Fig. 3). The distance between the α carbons of these residues, averaged over the six connexin subunits of the connexon, was derived from 100 ns of equilibrium molecular

Downloaded from http://hmg.oxfordjournals.org/ by guest on September 28, 2015

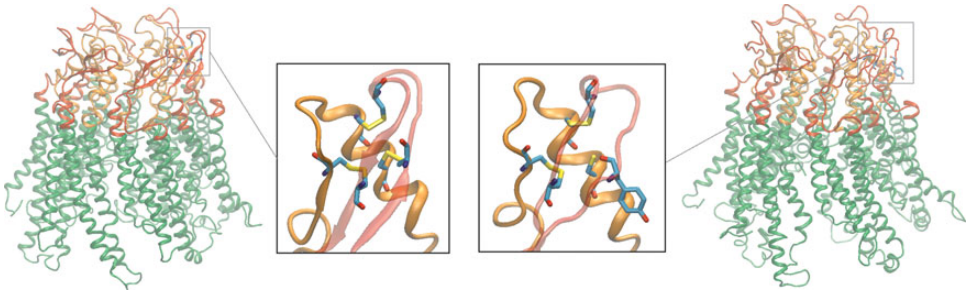

Figure 3. Cartoon representation of Cx26WT (left) and Cx26C169Y (right) hemichannels. The six connexins composing the hemichannels are drawn in ribbon; the extracellular loops (EC1 and EC2) are shown in orange and red (respectively). The insets show details of a single connexin; residues 53–180, 60–174 and 64–169, which in the wild-type structure are linked by disulfide bonds, are drawn in licorice representation.

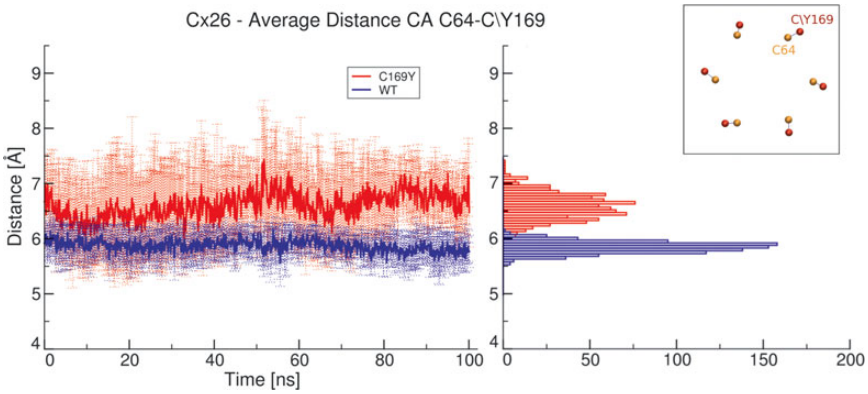

Figure 4. Distance between residues 64 and 169 during molecular dynamics simulation. The graph on the left shows average distances between α carbons of the two residues (inset) for the Cx26WT hemichannel (blue) and the Cx26C169Y hemichannel (red) as a function of time. Frequency histograms for the distribution of distance values are presented in the right panel. The absence of the disulfide bridge in the mutant results in a broader distribution, which is also shifted toward larger values.

dynamics and plotted as a function time in Figure 4 (left). Figure 4 (right) shows frequency histograms of distance distributions for the wild-type and the mutant connexon. The p.Cys169Tyr substitution modifies the mean value and the variance of these distributions, from 5.9 ± 0.2 Å for the wild-type to 6.6 ± 0.1 Å for the mutant. Although small, this difference (i) is statistically significant ($P < 0.0001$, Student's *t*-test) and (ii) alters the structure of the hemichannel in the extracellular region (particularly the E2 loop). Visual inspection of the molecular dynamics trajectories revealed a remarkable deformation affecting two of the proteins of the hexameric assembly. Albeit less pronounced, deformations were detectable also in the remaining four connexins.

To keep track of this diversity, we analyzed the trajectory of each protomer independently. First, we clustered the trajectory of the six connexins as described in the Materials and Methods section. Then, for each connexin, we selected one configuration for the mutant and two configurations for the wild-type as the most representative of their respective trajectories. We finally computed the root mean squared deviation (RMSD) of the atoms in the main chain of the seven residues (Asn54, Leu56, Gln57, Lys168, Asn176, Thr177, Asp179) that are considered responsible for the extracellular docking of the two connexons (2), taking the corresponding coordinates of the 3.5 Å X-ray crystallographic structure as reference. Compared with Cx26WT, the positions of these crucial residues in Cx26C169Y depart significantly more from those taken as reference (Fig. 5). The difference is caused by the displacement of the E2 loop in three of the six connexins. Indeed, if we concentrate only on residues Asn176 and Thr177, it is clear that the RMSD in three of the six mutant connexin exceeds 2.5 Å (Fig. 5, red diamonds), whereas the maximum RMSD in the wild-type is ~1.5 Å (Fig. 5, blue squares). We conclude that such departure from the crystallographic positions hinders the correct docking of the connexons and prevents the formation of a full gap junction channel.

Discussion

As is well known, not everyone with a given pathological mutation will eventually develop a related disease. One of the possible explanations could be reduced penetrance, but also the presence of modifier genes or other unknown elements in the genome may play a role (25). On the other hand, there is a large collection of variants of unknown significance occurring in patients. To assess the pathogenic role of these mutations, prediction tools are limited, in that they can only estimate the potential impact of a specific variation.

With specific regard to hereditary hearing loss, the analysis of several families has revealed a lack of segregation of a given allele with the clinical status (i.e. carriers who are in some cases healthy in others affected).

For example, the p.Met34Thr missense mutation of Cx26 was described first as an autosomal-dominant mutation (26), consistent with a subsequent study that reported to exert a dominant-negative effect over Cx26WT in *Xenopus* oocyte assays (27). p.Met34Thr was then re-classified as a polymorphism on the basis of contrasting functional data and lack of segregation with a hearing phenotype in some families (28). Subsequent work combining genetic, clinical, biochemical, electrophysiological and

Downloaded from http://hmg.oxfordjournals.org/ by guest on September 28, 2015

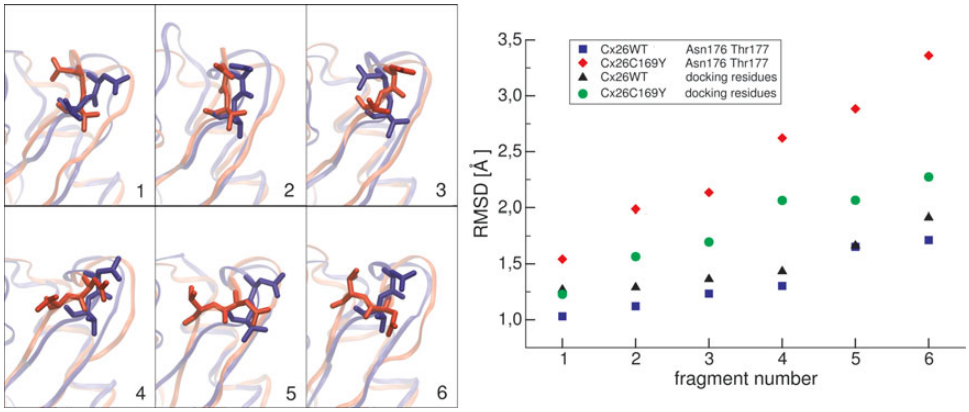

Figure 5. The p.Cys169Tyr mutation of Cx26 perturbs also residues that are considered critical for hemichannel docking and formation of a full gap junction channel. The six left panels show the orientation of side chains of residues Asn176 and Thr177 in the six connexins of the most representative configurations of wild-type (blue) and mutant (red) hemichannels. Structural alteration in the extracellular loop due to the absence of one of the disulfide bridges alters the position of the side chains of these two critical residues in the mutant hemichannel, which are thought to be responsible of the formation a full gap junction channel. The six panels are ranked in order of increasing RMSD of α carbons of Asn176 and Thr177 from the crystal structure of (2). The RMSD values for these two residues are reported in the graph of the right (blue squares for Cx26WT, red diamonds for Cx26C169Y), together with those of all the seven residues that have been identified as responsible for the docking in (2): Asn54, Leu56, Gln57, Lys168, Asn176, Thr177, Asp179 (black triangles for Cx26WT, green circles for Cx26C169Y). The positions of residues Asn176 and Thr177 are the most affected by the mutation. The values reported for Cx26WT are weighted averages over the two most representative configurations, as explained in the Materials and Methods section.

structural modeling studies, contributed to re-affirm the pathogenicity of this allele (22,29). Similarly, the p.Val37Ile variant of Cx26 has been initially reported as non-pathogenic. However, further analyses have documented an association of this variant with mild hearing loss in 9 of 10 genotypic combinations (30), in accord with other studies of the allele (31–35).

The p.Cys169Tyr variant of Cx26 analyzed here was also found to segregate only in some families/cases despite being classified as highly damaging by *in silico* predictor tools. Among the families we analyzed (*a*, *b* and *c*), the genotype–phenotype discordance and the results of our combined approach (Linkage and WES studies) showing p.Cys169Tyr of Cx26 as the only causative variant, prompted us to further investigate its role.

Cys169 is one of the six extracellular cysteine residues which are conserved in all connexin isoforms. These six cysteines form three disulfide bridges, which are likely to play an important role in guiding the correct folding of the connexin protein and the docking of the two hexameric hemichannels in the extracellular region. In the closely related connexin 32 protein (Cx32), the substitution of Cys64, which forms the disulfide bridge with Cys168 (the analogous of Cys169 in Cx26), with a serine generates a mutant protein that fails to form gap junction channels, even though it is correctly targeted to the cell membrane (36). Substitution of any one of the six cysteines to serine in Cx32 resulted in loss of channel conductance in paired *Xenopus* oocyte experiments (37,38).

Our experimental data, based on immunofluorescence of connexin proteins in HeLa DH cell transfectants (Fig. 2), strongly suggest that the mutated protein is correctly trafficked to the plasma membrane but fails to form gap-junction plaques, confirming that the extracellular cysteine pattern is fundamental for the docking of opposing hemichannels. The publication of the Cx26 full channel X-ray structure (2), and subsequent molecular dynamics simulations (24) demonstrated that the extracellular domain is rather stable. The pattern of disulfide bonds generated by the six cysteine residues present in the extracellular loops of Cx26 is clearly central to maintaining structural stability of this domain.

The analysis of molecular dynamics trajectory presented in this paper supports the notion that the p.Cys169Tyr mutation hinders the docking of Cx26 hemichannels by altering protein structure in the extracellular domain. In particular, we predict a significant displacement of two of the seven amino acids that are responsible for hemichannel docking, namely Asn176 and Thr177. It is worth noting that this alteration is not identical in all six connexins composing this hemichannel (Fig. 5) and, in some of the protomers, the structure remains virtually unaltered. We suspect that this discrepancy is due to the relative shortness of the simulated time span, and that a longer simulation would lead to similar configurations in all six connexins. In this vein, although a 100 ns molecular dynamics simulation is sufficient to re-equilibrate a protein structure in the proximity of a local energy minimum, detecting a structural rearrangement may require a longer simulation interval. Nonetheless, our results strongly suggest the extracellular domain of Cx26 is compromised by the p.Cys169Tyr mutation. In the absence of a co-expressed Cx26WT protein, or possibly another connexin (e.g. Cx30), the conformational change will eventually prevent correct docking of opposing hemichannels.

In conclusion, we believe that the approach used here elucidates the molecular pathogenesis of hereditary hearing loss and facilitates the understanding of the p.Cys169Tyr variant of Cx26 in both healthy and affected individuals. These results may pave the way to similar analyses of other diseases involving gap junction proteins.

Materials and Methods

Molecular genetics and audiometry

A series of consanguineous Qatari families were enrolled through the registry of the National Screening Program for the Early Detection of Hearing Loss (NSP-EDHL) at the Audiology Unit of Hamad Medical Hospital in Doha, Qatar. All patients provided written informed consent prior to DNA analysis and in the case of children, the consent was given by the parent/legal guardian. Hearing tests were performed through tonal audiometry using air conduction at 250, 500, 1000, 2000, 4000, 6000 and 8000 Hz. A clinical and dysmorphological examination of the patients was carried out to exclude non-genetic causes of hearing impairment. All analyzed patients were characterized by non-syndromic, congenital, sensorineural bilateral mild to severe hearing loss.

Downloaded from http://hmg.oxfordjournals.org/ by guest on September 28, 2015

DNA was extracted from peripheral blood collected in EDTA-containing tubes (Qiagen, USA). The promoter, the coding region and part of intron 1 (IVS1+1 G to A and -3170 G to A) were tested for mutations through PCR and Sanger sequencing. The presence of *GJB6* deletion (D13S1830) and the mitochondrial A1555G mutation were also tested.

Molecular cloning and mutagenesis

The coding region of the wild-type Cx26 was directionally cloned into the pIRES2 DsRed-Express2 vector between the *Xho*I/*Eco*RI restriction sites. The point mutation c.506G>A, leading to p.Cys169Tyr, was inserted by site-directed mutagenesis of the wild-type construct using the QuikChange Site-Directed Mutagenesis Kit (Agilent, Catalog # 200518). The mutagenesis protocol was performed using the manufacturer instructions and the following primers:

C169Yfor 5′-GCAGCGGCTGGTGAAGTACAACGCCTGGCCTTG-3′
C169Y rew 5′-CAAGGCCAGGCGTTGTACTTCACCAGCCGC TGC-3′.

The presence of the point mutation in the coding sequence was verified by sequencing. No additional mutations were detected.

Cx26 immunoreactivity in Hela cells

Hela DH cells (Sigma, cat. 96112022) were grown in DMEM (Gibco, catalog no. 41965-039) supplemented with 10% FBS (Gibco, catalog no. 10106169), plated on glass coverslips. Using Lipofectamine 3000, cells were transfected with either wild-type or mutated connexin constructs in order to overexpress, respectively, Cx26WT or Cx26C169Y proteins. Twenty-four hours after transfection, cells were fixed in 2% paraformaldehyde, saturated and permeabilized for 30 min in BSA 2% Tween 0.1% and incubated over night with a primary antibody against Cx26 (2.5 µg/ml, Connexin 26 Polyclonal Antibody, Rabbit, Invitrogen Catalog Number 71-0500) dissolved in BSA 1% (rinse solution). After three washes in rinse solution, cells were incubated with a secondary antibody [5 µg/ml, Alexa Fluor® 488 Goat Anti-Rabbit IgG (H + L), Invitrogen, Catalog Number A-11008]. After three further washes in rinse solution, glass coverslips with adherent cells were mounted with Fluor Save™ Reagent (Calbiochem, Cat # 345789) on a glass microscope slide. Cell preparations were analyzed using a confocal microscope (TCS SP5, Leica) equipped with an oil-immersion objective (63 × HCX PL APO 1.4 N.A., Leica). Laser line intensities and detector gains were carefully adjusted to minimize signal bleed through outside the designated spectral windows.

Molecular dynamics simulations

We already generated and published (24) a molecular dynamics model of a Cx26WT connexon in which the initial α carbon (C^{α}) positions were derived from the 3.5 Å X-ray crystallographic structure (protein data bank entry 2ZW3 (2)). Here, we generated a model of the Cx26C169Y mutant connexon from an equilibrium configuration of the Cx26WT model. To this end, we replaced Cys169 with a tyrosine in each of the six connexin protomers using the *mutate* tool of the Swiss PDB-Viewer (39). We then inserted the mutant connexon in a plasma membrane formed by 494 1-palmitoyl-2-oleoyl-sn-glycero-3-phosphocholine (POPC) molecules, as described in Pantano *et al.* (40). To speed up convergence of the interactions between proteins and membrane, coordinates for the original phospholipid bilayer were obtained from an equilibrium configuration of the membrane model described in (41). The system was then solvated with full-atom TIP3P water. Finally, Cl^- and K^+ ions were added at a concentration of ~0.15 M to neutralize the positive net charge of the connexon and to mimic a physiological ionic strength.

For both Cx26WT and Cx26C169Y models, the entire system comprised > 2×10^5 atoms and was equilibrated by a 100 ns molecular dynamics simulation using the GROMACS 4.6 software (42) and the Amber03 force field (43) in the NPT ensemble. As previously noted (22–24), a 100 ns simulation is sufficient to achieve a reasonably stable state. Temperature *T* and pressure *P* were kept constant, at 300 K and 1 atm, respectively, using the Berendsen thermostat and barostat (44). Fast smooth Particle-Mesh Ewald summation (45) was used for long-range electrostatic interactions, with a cut-off of 1.0 nm for the direct interactions. Simulations were performed under periodic boundary conditions using unitary boxes of 12 × 12 × 11 nm for both systems, consistent with the channel density measured in a Cx26 gap-junction plaque by atomic force microscopy (46).

Clustering of atomic configurations

A consolidated technique used to analyze long molecular dynamics trajectory and reduce data complexity while retaining the relevant information consists in clustering atomic configurations using suitable metrics (47). Here, clusters were obtained with the *g_cluster* tool of GROMACS 4.6 by restricting the analysis to the two extracellular loops (residues 41–75 and 155–192) of the six different connexins. Each cluster contained all the configurations for which the RMSD of the corresponding main-chain atoms was ≤1.1 Å. For the Cx26C169Y model, the single most important cluster contained 69.8% of the MD trajectory. For the Cx26WT model, instead, we obtained two principal clusters representing 46.0 and 17.0% of the configurations, respectively. The mean values of the observables reported in the Results section for Cx26WT are weighted averages of these two clusters, with weights proportional to the percentage of trajectory covered.

Acknowledgements

Computer simulations were performed at the CINECA supercomputer centers, and on a local workstation. We gratefully acknowledge the support of NVIDIA Corporation for the donation of the Tesla K40 GPU used for this research.

Conflict of Interest statement. The research was conducted in the absence of any commercial or financial relationships that could be construed as a potential conflict of interest.

Funding

This study was supported by QNRF (7th cycle NPRP7-583-3-156 to P.G. and K.H.) and Fondazione Telethon grant GGP13114 to F.M. Funding to pay the Open Access publication charges for this article was provided by the Fondazione Telethon, Italy.

References

1. Sohl, G. and Willecke, K. (2003) An update on connexin genes and their nomenclature in mouse and man. *Cell. Commun. Adhes.*, **10**, 173–180.
2. Maeda, S., Nakagawa, S., Suga, M., Yamashita, E., Oshima, A., Fujiyoshi, Y. and Tsukihara, T. (2009) Structure of the connexin 26 gap junction channel at 3.5 A resolution. *Nature*, **458**, 597–602.

Downloaded from http://hmg.oxfordjournals.org/ by guest on September 28, 2015

3. Oshima, A. (2014) Structure and closure of connexin gap junction channels. *FEBS Lett.*, **588**, 1230–1237.
4. Harris, A.L. (2007) Connexin channel permeability to cytoplasmic molecules. *Prog. Biophys. Mol. Biol.*, **94**, 120–143.
5. Goodenough, D.A. and Paul, D.L. (2009) Gap junctions. *Cold Spring Harb. Perspect. Biol.*, **1**, a002576.
6. Goldberg, G.S., Valiunas, V. and Brink, P.R. (2004) Selective permeability of gap junction channels. *Biochim. Biophys. Acta*, **1662**, 96–101.
7. Evans, W.H., De Vuyst, E. and Leybaert, L. (2006) The gap junction cellular internet: connexin hemichannels enter the signalling limelight. *Biochem. J.*, **397**, 1–14.
8. Saez, J.C. and Leybaert, L. (2014) Hunting for connexin hemichannels. *FEBS Lett.*, **588**, 1205–1211.
9. Forge, A., Becker, D., Casalotti, S., Edwards, J., Marziano, N. and Nevill, G. (2003) Gap junctions in the inner ear: comparison of distribution patterns in different vertebrates and assessment of connexin composition in mammals. *J. Comp. Neurol.*, **467**, 207–231.
10. Nickel, R. and Forge, A. (2008) Gap junctions and connexins in the inner ear: their roles in homeostasis and deafness. *Curr. Opin. Otolaryngol. Head Neck Surg.*, **16**, 452–457.
11. del Castillo, F.J. and del Castillo, I. (2011) The DFNB1 subtype of autosomal recessive non-syndromic hearing impairment. *Front. Biosci.-Landmrk*, **16**, 3252–3274.
12. Yilmaz, A. (2014) Bioinformatic analysis of GJB2 gene missense mutations. *Cell Biochem. Biophys.*, doi: 10.1007/s12013-014-0385-7.
13. Martin, P.E., Easton, J.A., Hodgins, M.B. and Wright, C.S. (2014) Connexins: sensors of epidermal integrity that are therapeutic targets. *FEBS Lett.*, **588**, 1304–1314.
14. Cryns, K., Orzan, E., Murgia, A., Huygen, P.L., Moreno, F., del Castillo, I., Chamberlin, G.P., Azaiez, H., Prasad, S., Cucci, R.A. *et al.* (2004) A genotype–phenotype correlation for GJB2 (connexin 26) deafness. *J. Med. Genet.*, **41**, 147–154.
15. Pfenniger, A., Wohlwend, A. and Kwak, B.R. (2011) Mutations in connexin genes and disease. *Eur. J. Clin. Invest.*, **41**, 103–116.
16. Azaiez, H., Chamberlin, G.P., Fischer, S.M., Welp, C.L., Prasad, S.D., Taggart, R.T., del Castillo, I., Van Camp, G. and Smith, R.J. (2004) GJB2: the spectrum of deafness-causing allele variants and their phenotype. *Hum. Mutat.*, **24**, 305–311.
17. Khalifa Alkowari, M., Girotto, G., Abdulhadi, K., Dipresa, S., Siam, R., Najjar, N., Badii, R. and Gasparini, P. (2012) GJB2 and GJB6 genes and the A1555G mitochondrial mutation are only minor causes of nonsyndromic hearing loss in the Qatari population. *Int. J. Audiol.*, **51**, 181–185.
18. Birkenhager, R., Prera, N., Aschendorff, A., Laszig, R. and Arndt, S. (2014) A novel homozygous mutation in the EC1/EC2 interaction domain of the gap junction complex connexon 26 leads to profound hearing impairment. *BioMed Res. Int.*, **2014**, 307976.
19. Schwarz, J.M., Rodelsperger, C., Schuelke, M. and Seelow, D. (2010) MutationTaster evaluates disease-causing potential of sequence alterations. *Nat. Methods*, **7**, 575–576.
20. Adzhubei, I., Jordan, D.M. and Sunyaev, S.R. (2013) Predicting functional effect of human missense mutations using PolyPhen-2. *Curr. Protoc. Hum. Genet.*, Chapter 7, Unit7 20.
21. Ng, P.C. and Henikoff, S. (2003) SIFT: predicting amino acid changes that affect protein function. *Nucleic Acids Res.*, **31**, 3812–3814.
22. Zonta, F., Buratto, D., Cassini, C., Bortolozzi, M. and Mammano, F. (2014) Molecular dynamics simulations highlight structural and functional alterations in deafness-related M34T mutation of connexin 26. *Front. Physiol.*, **5**, 85.
23. Zonta, F., Polles, G., Sanasi, M.F., Bortolozzi, M. and Mammano, F. (2013) The 3.5 angstrom X-ray structure of the human connexin26 gap junction channel is unlikely that of a fully open channel. *Cell Commun. Signal.*, **11**, 15.
24. Zonta, F., Polles, G., Zanotti, G. and Mammano, F. (2012) Permeation pathway of homomeric connexin 26 and connexin 30 channels investigated by molecular dynamics. *J. Biomol. Struct. Dyn.*, **29**, 985–998.
25. Cooper, D.N., Krawczak, M., Polychronakos, C., Tyler-Smith, C. and Kehrer-Sawatzki, H. (2013) Where genotype is not predictive of phenotype: towards an understanding of the molecular basis of reduced penetrance in human inherited disease. *Hum. Genet.*, **132**, 1077–1130.
26. Kelsell, D.P., Dunlop, J., Stevens, H.P., Lench, N.J., Liang, J.N., Parry, G., Mueller, R.F. and Leigh, I.M. (1997) Connexin 26 mutations in hereditary non-syndromic sensorineural deafness. *Nature*, **387**, 80–83.
27. Skerrett, I.M., Di, W.L., Kasperek, E.M., Kelsell, D.P. and Nicholson, B.J. (2004) Aberrant gating, but a normal expression pattern, underlies the recessive phenotype of the deafness mutant Connexin26M34T. *FASEB J.*, **18**, 860–862.
28. Feldmann, D., Denoyelle, F., Loundon, N., Weil, D., Garabedian, E.N., Couderc, R., Joannard, A., Schmerber, S., Delobel, B., Leman, J. *et al.* (2004) Clinical evidence of the nonpathogenic nature of the M34T variant in the connexin 26 gene. *Eur. J. Hum. Genet.*, **12**, 279–284.
29. Bicego, M., Beltramello, M., Melchionda, S., Carella, M., Piazza, V., Zelante, L., Bukauskas, F.F., Arslan, E., Cama, E., Pantano, S. *et al.* (2006) Pathogenetic role of the deafness-related M34T mutation of Cx26. *Hum. Mol. Genet.*, **15**, 2569–2587.
30. Snoeckx, R.L., Huygen, P.L., Feldmann, D., Marlin, S., Denoyelle, F., Waligora, J., Mueller-Malesinska, M., Pollak, A., Ploski, R., Murgia, A. *et al.* (2005) GJB2 mutations and degree of hearing loss: a multicenter study. *Am. J. Hum. Genet.*, **77**, 945–957.
31. Abe, S., Usami, S., Shinkawa, H., Kelley, P.M. and Kimberling, W.J. (2000) Prevalent connexin 26 gene (GJB2) mutations in Japanese. *J. Med. Genet.*, **37**, 41–43.
32. Wilcox, S.A., Saunders, K., Osborn, A.H., Arnold, A., Wunderlich, J., Kelly, T., Collins, V., Wilcox, L.J., McKinlay Gardner, R.J., Kamarinos, M. *et al.* (2000) High frequency hearing loss correlated with mutations in the GJB2 gene. *Hum. Genet.*, **106**, 399–405.
33. Kenna, M.A., Wu, B.L., Cotanche, D.A., Korf, B.R. and Rehm, H.L. (2001) Connexin 26 studies in patients with sensorineural hearing loss. *Arch. Otolaryngol. Head Neck Surg.*, **127**, 1037–1042.
34. Lin, D., Goldstein, J.A., Mhatre, A.N., Lustig, L.R., Pfister, M. and Lalwani, A.K. (2001) Assessment of denaturing high-performance liquid chromatography (DHPLC) in screening for mutations in connexin 26 (GJB2). *Hum. Mutat.*, **18**, 42–51.
35. Marlin, S., Garabedian, E.N., Roger, G., Moatti, L., Matha, N., Lewin, P., Petit, C. and Denoyelle, F. (2001) Connexin 26 gene mutations in congenitally deaf children: pitfalls for genetic counseling. *Arch. Otolaryngol. Head Neck Surg.*, **127**, 927–933.
36. Oshima, A., Doi, T., Mitsuoka, K., Maeda, S. and Fujiyoshi, Y. (2003) Roles of Met-34, Cys-64, and Arg-75 in the assembly of human connexin 26. Implication for key amino acid residues for channel formation and function. *J. Biol. Chem.*, **278**, 1807–1816.
37. Dahl, G., Levine, E., Rabadan-Diehl, C. and Werner, R. (1991) Cell/cell channel formation involves disulfide exchange. *Eur. J. Biochem./FEBS*, **197**, 141–144.
38. Dahl, G., Werner, R., Levine, E. and Rabadan-Diehl, C. (1992) Mutational analysis of gap junction formation. *Biophys. J.*, **62**, 172–180; discussion 180–182.

Downloaded from http://hmg.oxfordjournals.org/ by guest on September 28, 2015

39. Guex, N. and Peitsch, M.C. (1997) SWISS-MODEL and the Swiss-PdbViewer: an environment for comparative protein modeling. *Electrophoresis*, **18**, 2714–2723.
40. Pantano, S., Zonta, F. and Mammano, F. (2008) A fully atomistic model of the Cx32 connexon. *PloS One*, **3**, e2614.
41. Pantano, S. and Carafoli, E. (2007) The role of phosphorylation on the structure and dynamics of phospholamban: a model from molecular simulations. *Proteins*, **66**, 930–940.
42. Hess, B., Kutzner, C., van der Spoel, D. and Lindahl, E. (2008) GROMACS 4: algorithms for highly efficient, load-balanced, and scalable molecular simulation. *J. Chem. Theory Comput.*, **4**, 435–447.
43. Duan, Y., Wu, C., Chowdhury, S., Lee, M.C., Xiong, G., Zhang, W., Yang, R., Cieplak, P., Luo, R., Lee, T. *et al.* (2003) A point-charge force field for molecular mechanics simulations of proteins based on condensed-phase quantum mechanical calculations. *J. Comput. Chem.*, **24**, 1999–2012.
44. Berendsen, H.J.C., Postma, J.P.M., van Gunsteren, W.F., Dinola, A. and Haak, J.R. (1984) Molecular dynamics with coupling to an external bath. *J. Chem. Phys.*, **81**, 3684–3690.
45. Darden, T., York, D. and Pedersen, L. (1993) Particle mesh Ewald: an N·log(N) method for Ewald sums in large systems. *J. Chem. Phys.*, **98**, 10089–10093.
46. Muller, D.J., Hand, G.M., Engel, A. and Sosinsky, G.E. (2002) Conformational changes in surface structures of isolated connexin 26 gap junctions. *EMBO J.*, **21**, 3598–3607.
47. Karpen, M.E., Tobias, D.J. and Brooks, C.L. III (1993) Statistical clustering techniques for the analysis of long molecular dynamics trajectories: analysis of 2.2-ns trajectories of YPGDV. *Biochemistry*, **32**, 412–420.

Downloaded from http://hmg.oxfordjournals.org/ by guest on September 28, 2015